# Correlation between arterial blood volume obtained by arterial spin labelling and cerebral blood volume in intracranial tumours.

van Westen, Danielle; Petersen, Esben T; Wirestam, Ronnie; Siemund, Roger; Markenroth Bloch, Karin; Ståhlberg, Freddy; Björkman-Burtscher, Isabella; Knutsson, Linda

*Published in:*
Magma

*DOI:*
10.1007/s10334-011-0255-x

2011

# Correlation between arterial blood volume obtained by arterial spin labelling and cerebral blood volume in intracranial tumours

Danielle van Westen MD, PhD[1, 2], Esben T. Petersen, PhD[3], Ronnie Wirestam PhD[4], Roger Siemund MD, PhD[1, 2], Karin Markenroth Bloch PhD[5], Freddy Ståhlberg, PhD[1, 4], Isabella M. Björkman-Burtscher MD, PhD[1, 2], Linda Knutsson, PhD[4]

(1) Department of Diagnostic Radiology, Lund University, Lund, Sweden
(2) Center for Medical Imaging and Physiology, Skåne University Hospital, Lund, Sweden
(3) Department of Radiology, University Medical Center Utrecht, Utrecht, The Netherlands
(4) Department of Medical Radiation Physics, Lund University, Lund, Sweden,
(5) Philips Medical Systems, Lund, Sweden

Corresponding author:
Danielle van Westen
Dept of Radiology
Lund University Hospital
SE – 221 85 Lund, Sweden
Tel: +46 +46 175108
FAX: +46 +46 121837
E-mail: danielle.van_westen@med.lu.se

**Short Title:** Arterial blood volume in intracranial tumours

Number of figures: 5
Number of tables: 2
Number of references: 38

**Abstract**

***Objective:*** To compare measurements of the arterial blood volume (aBV), a perfusion parameter calculated from arterial spin labelling (ASL), and cerebral blood volume (CBV), calculated from dynamic susceptibility contrast (DSC) MRI. In the clinic, CBV is used for grading of intracranial tumours

***Materials and methods***: Estimates of aBV from the model-free ASL technique quantitative STAR labelling of arterial regions (QUASAR) experiment and of DSC-CBV were obtained at 3T in ten patients with eleven tumours (three grade III gliomas, four glioblastomas and four meningiomas, two in one patient). Parametric values of aBV and CBV were determined in the tumour as well as in normal grey matter (GM), and tumour-to-GM aBV and CBV ratios were calculated.

***Results:*** In a 4-pixel ROI representing maximal tumour values, the coefficient of determination $R^2$ was 0.61 for the comparison of ASL-based aBV tumour-to-GM ratios and DSC-MRI-based CBV tumour-to-GM ratios and 0.29 for the comparison of parametric values of ASL-aBV and DSC-CBV, under the assumption of proportionality. Both aBV and CBV showed a non-significant tendency to increase when going from grade III gliomas to glioblastomas to meningiomas.

***Conclusion:*** These results suggest that measurement of aBV is a potential tool for non-invasive assessment of blood volume in intracranial tumours.

**Keywords**

brain tumour; blood volume; arterial spin labelling; dynamic susceptibility contrast MRI;

## Introduction

Gliomas are the most common primary tumours of the brain, with astrocytomas being the most common subtype. Astrocytoma grading is important for determining both prognosis and therapy. Vascular morphology is a critical parameter in assessing malignant potential and survival, since tumour growth beyond 1 to 2 mm largely depends on the development of adequate vascular supply [1]. Brain tumours disrupt the integrity of the blood brain barrier (BBB) and exhibit other pathological features, including marked angiogenesis with endothelial proliferation, severe hypoxia and tumour necrosis [2-4]. The degree of tumour angiogenesis and capillary permeability can be assessed by bolus-tracking perfusion MRI measurements, for example, dynamic susceptibility contrast magnetic resonance imaging (DSC-MRI). Several studies have shown a statistically strong correlation between tumour cerebral blood volume (CBV) and astrocytoma grading [5, 6], as well as between tumour CBV and conventional angiographic tumour vascularity [7] with the exception of oligodendrogliomas that may display elevated tumour CBV not reflective of high grade histopathology [8].

In DSC-MRI, CBV is assumed to be proportional to the area under the contrast agent concentration-time curve [9], but the technique does not normally yield reliable results in absolute terms. As an alternative to DSC-MRI, with regard to cerebral blood flow (CBF) quantification, arterial spin labelling (ASL) techniques have shown considerable potential [10-13]. ASL does not require injection of contrast agent and is thus completely non-invasive. Amongst recent developments, a dynamic model-free ASL technique, named quantitative STAR labelling of arterial regions (QUASAR), has been proposed for quantification of CBF based on deconvolution [14]. With the QUASAR technique, images are acquired at different inversion times after labelling, thereby allowing for the whole signal difference curve over time to be determined. Because ASL is based on measurement of a diffusible tracer, the technique does not allow for determination of CBV. Instead, the volume of blood in arteries and arterioles (aBV), with a velocity exceeding a predefined threshold is calculated as the total area of the arterial signal curve divided by the bolus area. This parameter is named the arterial blood volume (aBV) and its magnitude is expressed in percent of the voxel volume. The cerebral blood volume (CBV) is the sum of the aBV and the capillary and venous blood volumes.

Measurement of CBV without the use of contrast agents is interesting from a clinical point of view, firstly because this allows for comparison of repeated measurements, for example, during the course of treatment. Secondly, the possible link between renal insufficiency and nephrogenic systemic fibrosis implies a demand for non-contrast-agent based assessment of the cerebral microcirculation [15].

The aim of the present study was to investigate the correlation between aBV and CBV in intracranial tumours as a first step in the process of evaluating the use of aBV as a tool for tumour grading similar to existing CBV-based methods. We compared tumour-to-healthy grey matter ratios as well as absolute estimates of aBV and CBF obtained by ASL to those from CBV and CBF obtained by DSC-MRI in ten patients with three types of brain tumours.

## Materials and methods

***Materials:*** Ten subjects with intracranial tumours (three grade III gliomas, four glioblastomas and four meningiomas, two in one patient) were included in the study. In all patients, a contrast-enhancing lesion was present on post-contrast T1-weighted images. All gliomas were biopsy-proven. In the meningiomas, diagnosis was based on the typical imaging findings of an extra-axial homogenously enhancing mass lesion with dural extension. Four of the patients were men and the median age of all patients was 49 years (range 35 - 68 years).

The study was approved by the local ethics committee and written informed consent was obtained from all patients.

***Image acquisition:*** MRI examinations were performed using a 3T scanner (Philips Achieva®, Philips Medical Systems, Best, The Netherlands) and included ASL (QUASAR) and DSC-MRI. ASL images were obtained with crushed arterial signal using a velocity-encoding gradient (crushed data) as well as with retained arterial signal (non-crushed data). Two flip angles were used to obtain equilibrium magnetization in blood. QUASAR parameters were TR/TE/$\Delta$TI/TI1=4000/23/300/40 ms, matrix=64×64, seven slices (6 mm thickness/2 mm slice gap), FOV=240 mm, flip angles=35/11.7°, SENSE factor 2.5, Venc=[∞ ,4 cm/s], and 82 averages (48 using Venc=4 cm/s, 24 using Venc=∞, 10 with smaller flip angle), implemented in a single pulse sequence. For DSC-MRI, gradient echo EPI was used with TR/TE=1360/29 ms, flip angle=90°, 23 slices (5 mm thickness/1 mm gap), FOV=220 mm, matrix=128×128 and SENSE factor 2.5. A bolus (injection rate 5 ml/s) of 0.1

mmol/kg bodyweight gadolinium-based contrast agent (Dotarem®, Guerbet, Paris, France) was administered and followed by a saline flush.

Acquisition time was roughly 5 min for ASL and 1.5 min for DSC, in-plane spatial resolution was 3.75 mm² for ASL and 1.7 mm² for DSC, and spatial coverage was 56 mm (6 mm slice thickness and 2 mm gap) for ASL and 138 mm (5 mm slice thickness and 1 mm gap) for DSC-MRI.

Morphological data included transversal and sagittal T2-weighted sequences (TR/TE=3000 ms/80 ms), a FLAIR sequence (TR=12000 ms/TE=140 ms/TI=2500 ms), transversal pre- and post-contrast T1-weighted sequences (TR=500ms/TE=10 ms) as well as a post-contrast coronal T1-weighted sequence.

***Data processing:*** For ASL, all perfusion maps obtained using QUASAR were calculated off-line using a computer program developed by one of the authors (E.T.P). A rejection algorithm was applied to exclude measurements influenced by excessive patient movement. By subtracting the crushed data from the non-crushed data, arterial signal curves were obtained. Arterial blood volume (aBV) was determined as the time integral of the arterial signal curve divided by the bolus area that corresponds to an initially labelled voxel with 100% blood volume:

$$aBV = \frac{\int_{-\infty}^{\infty} (\Delta M_{ncr}(t) - \Delta M_{cr}(t)) e^{\frac{t}{T_{1a}}} dt}{2 \cdot M_{a,0} \cdot \tau_b \cdot \alpha} \qquad (1)$$

where $T_{1a}$ is the longitudinal relaxation time of the blood, $\tau_b$ is the duration of the labelling and $\alpha$ is the inversion efficiency (set to 0.95 in our case). $\Delta M_{ncr}$ and $\Delta M_{cr}$ correspond to the non-crushed and crushed image data and $M_{a,0}$ to the equilibrium magnetization in blood. Deconvolution was performed using a block-circulant singular value decomposition (SVD) method [16]. CBF was calculated using arterial input functions (AIFs) selected from all ASL slices corresponding to an aBV threshold of 1.2% [14].

For DSC-MRI, CBV and CBF were calculated in pseudo-absolute terms, i.e. CBV was given by the tissue concentration time integral divided by the measured AIF time integral (not corrected for partial volume effects), and the obtained ratio was corrected for differences between capillary and arterial haematocrit values [17]. Calculation of CBF was based on the central volume theorem and Zierler's area–to–height relationship and accomplished by SVD deconvolution. Contrast agent leakage

in the tumour was corrected for using a linear fitting algorithm [18]. The software package 'nordicICE' (NordicNeuroLab, Bergen, Norway, http://www.nordicneurolab.com) was used to retrieve a global AIF from the middle cerebral artery (MCA) branches in the Sylvian-fissure region. This was done automatically by searching for concentration time curves that have the characteristics of an AIF.

***Data-analysis:*** The "ImageJ" software (ImageJ 1.37, plug-in "Sync Windows" by P. Kelly and improved by J. Walter, http://rsbweb.nih.gov/ij/) was used for evaluation of the aBV and CBF maps obtained by ASL as well as the CBF and CBV maps obtained by DSC-MRI. Firstly, the morphological information from the T2-weighted and contrast-enhanced T1-weighted sequences was used to localise the tumour. Special attention was paid to identify adjacent vessels in order to avoid subsequent inclusion of these in the ROI. Parametric maps from ASL were rescaled to the in-plane resolution used in DSC-MRI (voxel size 1.72 x 1.72 $mm^2$). According to the literature, the best reproducibility of CBV measurements is achieved when the highest CBV value obtained from repeated CBV measurements using small ROIs (4 pixels) is used for CBV assessment in tumour tissue [19]. Thus in our primary analysis, multiple ROIs of 4 pixels (11.8 $mm^2$) were placed on the DSC-CBV maps in the area where the CBV was maximally elevated according to visual assessment. The highest value thus obtained was used for calculation of the ratio between the tumour and healthy brain tissue. The same method was then used for measurement of the aBV. In practice, this implied that the location of the ROI could differ between CBV and aBV, as the pixels with the highest value for each parameter did not necessarily overlap and also slice position and thickness differed slightly between ASL and DSC-MRI. For comparison, aBV was also obtained at the site of the maximum CBV and CBV was obtained at the site of the maximum aBV (4-pixel ROIs in both cases). Measurements of ASL-CBF and DSC-CBF were performed in the same slice and tumour portion as those of aBV and DSC-CBV. Also in this case, the positions of the ROIs could differ from those used for measurement of aBV and DSC-CBV, depending on the location of the ROI with the highest value for blood volume and blood flow, respectively. Placement of ROIs was performed separately by two independent observers (DvW and LK), measurements were then reassessed by the observers together and a consensus was established. For comparison, measurements were also performed in a ROI covering the entire tumour in the same

slice as the 4-pixel ROI. Standard deviations of the average parametric value in the 4-pixel ROI and the ROI covering the whole tumour, respectively were calculated as parametric value and as percentage of the average parametric value in the ROI.

Grey matter (GM) was used as the healthy brain tissue reference. The GM perfusion parameters were calculated as follows: slices without any major inclusion of tumour were identified and the three DSC-MRI slices that best matched the two corresponding QUASAR slices were selected. In the QUASAR data, pixel values exceeding 3 times the mean CBF of the two ASL slices were excluded because patient movement can manifest itself as hyperintense regions in the CBF maps [20, 21]. These regions correspond to the water-fat shift artefact that may be present in the ASL images and that may persist even after subtracting the control and label images. To eliminate large-vessel contributions from the DSC-MRI CBF maps, all pixels with values exceeding two times the mean CBF of the three DSC-MRI slices were excluded [22]. In both cases, i.e. DSC-MRI and QUASAR-ASL, approximately 1 % of the data were discarded. Then, T1-based masks obtained from the QUASAR experiment were used for visualization of GM regions in order to extract GM aBV, CBF and CBV data from QUASAR and DSC-MRI maps. Mean GM aBV, CBF and CBV estimates were calculated over all included slices (ROI size approximately 30 $cm^2$). Finally, the ratio between tumour and healthy grey matter was calculated for all parameters, i.e., aBV, ASL-CBF, DSC-CBV, and DSC-CBF.

***Statistics:*** Medians were calculated for each tumour type. aBV versus DSC-CBV as well as ASL-CBF versus DSC-CBF were plotted for all selected ROIs. Linear-regression analyses, with and without the assumption of proportionality, provided the corresponding linear equations. Standard deviations of parametric values in the 4 pixel ROI were compared using the Wilcoxon matched pairs test. The level of significance was set at $P < 0.05$.

**Results**

Maps of aBV, DSC-CBV, ASL-CBF and DSC-CBF and the contrast-enhanced T1-weighted image from a meningioma and a glioblastoma (grade IV) are shown in Figures 1 and 2.

1. Tumour-to-GM ratios

Median tumour-to-GM ratios from the four perfusion parameters from the 4-pixel ROI as well as from the ROI covering the entire tumour in the same slice are displayed in Table 1. The observed trend was that an increase in aBV was accompanied by an increase in DSC-CBV when going from grade III gliomas to glioblastomas and from glioblastomas to meningiomas, although group sizes were too small to allow for statistical testing. A similar pattern was seen for ASL-CBF and DSC-CBF with the smallest values found in the grade III gliomas and the highest in the meningiomas. This trend was most obvious for the ratios from the 4-pixel ROI, representing the maximal tumour value, but was also present in the ratios based on the ROI covering the entire tumour.

When assuming proportionality between ASL-aBV and DSC-CBV ratios from the 4-pixel ROI, the coefficient of determination $R^2$ was 0.61 (Figure 3a). The corresponding comparison of CBF ratios showed a coefficient of determination of 0.86 (Figure 3b). Without the assumption of proportionality, the following linear relationships and coefficients of determination were observed:

$CBV(DSC)_{ratio} = 1.97\ aBV(ASL)_{ratio} + 0.42$ ($R^2 = 0.61$, $P = 0.0045$) and

$CBF(DSC)_{ratio} = 0.90\ CBF(ASL)_{ratio} + 0.10$ ($R^2 = 0.86$, $P = 0.0001$).

For the ROI covering the entire tumour, only the tumour-to-GM ratio of aBV and CBV are reported (Figure 3c). The coefficient of determination for the comparison of ASL-aBV and DSC-CBV ratios was 0.17, under the assumption of proportionality. Without the assumption of proportionality, the following linear relationship was observed:

$CBV(DSC)_{ratio} = 1.22\ aBV(ASL)_{ratio} + 1.16$ ($R^2 = 0.25$, $P = 0.12$)

2. Parametric values

Values (median and range) of each parameter per tumour type determined as the maximum value based on a 4-pixel ROI and the value in the entire tumour in one slice are given in Table 2. Similarly to the tumour-to-GM ratios, there was an increase in aBV and ASL-CBF, accompanied by an increase in DSC-

CBV and DSC-CBF, respectively, when going from grade III gliomas to glioblastomas and from glioblastomas to meningiomas. This increase was most obvious for the 4-pixel ROI representing maximal tumour values.

When assuming proportionality between ASL-aBV and DSC-CBV, the coefficient of determination was 0.29 for the 4-pixel ROI (Fig 4a). Under the same condition and for the same ROI, the coefficient of the determination for the comparison of ASL-CBF and DSC-CBF was 0.86 (Fig 4b). Without the assumption of proportionality, the following linear relationships and coefficients of determination were observed:

CBV(DSC)= 73 aBV(ASL) + 67 ($R^2$ = 0.37, *P* = 0.049 ) and

CBF(DSC)= 9.40 CBF(ASL) + 468 ($R^2$ = 0.86, *P* <0.0001) for the 4-pixel ROI

For the corresponding comparison of aBV and CBV for the ROI covering the entire tumour in the same slice the coefficient of determination of $R^2$ was -0.027 (Fig 4c). Without the assumption of proportionality, the relationship was:

CBV(DSC) =45 aBV(ASL) + 75 ($R^2$ = 0.16, *P* = 0.22).

Note that all DSC-based values are systematically overestimated, for reasons stated above, and should be regarded as CBV and CBF indices.

3. Standard deviation within the ROI

Standard deviations of the parametric values in the 4 pixel ROI and for the ROI covering the entire tumour are listed in Table 3, absolute value and percentage of the average value in the ROI. Median standard deviations for each parameter, all tumour types included, are given also.

Median standard deviations of the parameters were considerably smaller for the 4 pixel ROI as compared to the ROI covering the entire tumour in the slice, 15 % versus 55 % for ASL-aBV, 16 % versus 32 % for DSC-CBV, 10 % versus 57 % for ASL-CBF and 10 % versus 31 % for DSC-CBF. The range of the median standard deviation was highest for the aBV, 2 – 42 %, to be compared to 2 - 24 % for the CBV, however there was no significant difference between the standard deviations of aBV and CBV (*P* = 0.33, Wilcoxon matched pairs test).

4. Location dependence of tumour-to-GM ratios and parametric values

In seven patients (two grade III gliomas, three grade IV gliomas and two meningiomas) the 4-pixel area with maximum aBV overlapped the 4-pixel area with maximum CBV. In two patients (one meningioma and one grade III glioma) these areas were contingent, i.e. the areas were not exactly similar, but were in touch with each other. In one grade IV glioma and one meningioma patient, the 4-pixel areas with maximum aBV and maximum CBV were separated from each other. In the meningioma patient, the 4-pixel area with maximum aBV was located 2 cm from the 4-pixel area with maximum CBV in a 5.5 x 3 x 2.5 cm large tumour. In the patient with a grade IV glioma, the 4-pixel areas with maximum aBV and maximum CBV were separated from each other by 1.5 cm in a 5 x 4 x 4 cm large tumour.

For tumour-to-GM ratios of ASL-aBV and DSC-CBV measured in the 4-pixel ROI of the maximum ASL-aBV, the coefficient of determination was 0.55 under the assumption of proportionality (Fig 5 a). Similarly, for tumour-to-GM ratios of ASL-aBV and DSC-CBV measured in the 4-pixel ROI of the maximum DSC-CBV, the coefficient of determination was 0.50 under the assumption of proportionality (Fig 5 b). Without the assumption of proportionality, the following linear relationships and coefficients determination were observed for tumour-to-GM ratios:

$CBV(DSC)_{ratio} = 1.46\ aBV(ASL)_{ratio} + 0.50$ ($R^2 = 0.56$, $P = 0.008$) for the location of the maximum ASL-aBV and

$CBV(DSC)_{ratio} = 1.77\ aBV(ASL)_{ratio} + 0.39$ ($R^2 = 0.51$, $P = 0.014$) for the location of the maximum DSC-CBV.

For values of ASL-aBV and DSC-CBV measured in the 4-pixel ROI of the maximum ASL-aBV, the coefficient of determination was 0.30 under the assumption of proportionality (Fig 5c). Similarly, for ASL-aBV and DSC-CBV measured in the 4-pixel ROI of the maximum DSC-CBV, the coefficient of determination was 0.29 under the assumption of proportionality (Fig 5d). Without the assumption of proportionality, the following linear relationships and coefficients of determination were observed for the parametric values:

$CBV(DSC) = 59\ aBV(ASL) + 50$ ($R^2 = 0.37$, $P = 0.053$) for the location of the maximum ASL-aBV and

CBV(DSC) = 71 aBV(ASL) + 57 ($R^2$ = 0.33, $P$ = 0.013) for the location of the maximum DSC-CBV.

## Discussion

The present study is, to our knowledge, the first report on the ASL-based parameter aBV as a marker of CBV in brain tumour patients. Measurements of aBV and CBF from arterial spin labelling were compared to the corresponding parameters CBV and CBF from DSC-MRI in eleven tumours covering three types of intracranial tumours. Without the assumption of proportionality, ASL-aBV correlated well with DSC-CBV and the highest coefficient of determination was observed for tumour-to-brain ratios from a 4-pixel ROI representing the maximal values of the parameter of interest within the tumour ($R^2$ = 0.61, $P$ = 0.0045). A lesser but still satisfactory correlation was found for the comparison of aBV and CBV values ($R^2$ = 0.37, $P$ = 0.049). A potential difference in aBV between tumour types was found for ratios as well as parametric values, in the 4-pixel ROI as well as in the ROI covering the entire tumour, with an increase in aBV, being accompanied by an increase in DSC-CBV when going from grade III gliomas to glioblastomas and from glioblastomas to meningiomas. These results suggest that aBV holds promise to potentially be comparable to CBV as a tool for tumour grading similar to existing CBV-based methods, when the ratio between the maximum parametric value in 4-pixel ROI and healthy grey matter is used.

Determination of hemodynamic parameters such as the ASL-aBV using a 4-pixel ROI, is analoguous to well-established and validated routines for DSC-CBV estimation and was initially introduced for PET-measurements [23]. At histopathologic evaluation the highest degree of vascular hyperplasia has been found in the biopsy specimen with the highest maximum signal intensity in DSC-CBV [8]. Our finding that ratios and values obtained from a ROI covering the entire tumour did not correlate significantly ($R^2$ = 0.25, $P$ = 0.12 and $R^2$ = 0.16, $P$ = 0.22, Figures 3c and 4 c, respectively) may be explained by tumour heterogeneity and in some cases the presence of necrosis. Tumour heterogeneity may also explain the median standard deviations of the four parameters in the 4-pixel ROI, 10 - 16 %, being considerably smaller than in the ROI covering the entire tumour, 31-57 %, all tumours included (Table 3). The range of the median standard deviation in the 4-pixel ROI was largest for the aBV, 2 – 44 %, to be compared with 2 - 24 % for the CBV. This may be due to

a number of factors, such as the difference between physiological phenomenon measured by these two blood volumes. No obvious location dependence was found for lesion-to-GM ratios, that is measurement of parameters at the site of the maximum aBV or CBV correlated similarly ($R^2$ = 0.56, *P* = 0.008 for measurement in the area of the maximum aBV and $R^2$ = 0.51, *P* = 0.014 for measurement in the area of the maximum CBV, respectively). For parametric values of the maximum aBV or CBV ($R^2$ = 0.37, *P* = 0.053 for measurement in the area of the maximum aBV and $R^2$ = 0.33, *P* = 0.013 for measurement in the area of the maximum CBV, respectively) the relationships were less satisfactory.

Perfusion parameters can contribute to tumour grading, and DSC-MRI estimates have been shown to differ between high-grade and low-grade gliomas [5-8] and to be related to clinical outcome (survival time) [24]. Furthermore, ASL perfusion has consistently shown higher CBF values in high-grade than in low-grade gliomas [25-27]. However, the main parameter of interest is the CBV, depicting the overall tumour vascularity, which allows indirect assessment of tumour angiogenesis [5]. Measurement of CBV by DSC-MRI has been shown to correlate with both conventional angiographic assessments of tumour vascular density and histological measurements of tumour neovascularization [5-7]. Parenthetically, it should be mentioned that increased tumour vascularity is not always synonymous with malignancy since especially extraaxial neoplasms, e.g. meningiomas, can be highly vascular but rather benign in terms of biological behaviour.

Assessment of tumour blood volume using ASL would be of considerable clinical interest since ASL yields absolute values allowing for comparison between patients or comparison of intraindividual values obtained during treatment [28]. Also, the non-invasiveness of ASL, denoting its capacity to assess perfusion parameters without using contrast agent, is of clinical interest as it allows for repeated measurements in one session. Furthermore, the use of contrast agents is increasingly debated due to its possible relationship with nephrogenic systemic fibrosis [16]. ASL is, however, based on the measurement of a diffusible tracer, and thus does not allow for determination of CBV. Instead, the volume of the blood in arteries and arterioles with a velocity over a predefined threshold (4 cm/s in our case) is measured. This threshold is to be compared to the velocities in these vessels just proximal to the capillary bed, decreasing from 10 cm/s to 0.2 cm/s, suggesting that the arteries and

most of the arterioles are likely to be included in the measurement of aBV [29]. The average aBV value in healthy grey matter of 0.95 %, obtained in the present study, is well in line with previous QUASAR studies [22]. Furthermore, the arterial blood volume in the brain has been determined to be 37 % of the total blood volume using $H_2\ ^{15}O$ – PET [30]. The first-pass extraction fraction (EF) of $H_2\ ^{15}O$, a freely diffusible tracer, is less than 1 and the value for the arterial blood volume calculated by Ito et al. thus also includes a part of the intravascular volume of the capillary and vein. Assuming the EF to be 0.9, the true arterial fraction of CBV will be 30 % which corresponds to an aBV estimate of 0.93 %. However, Ito et al, did not observe any correlation between aBV and CBV in grey matter.

Angiogenesis in intracranial tumours leads to an increase of the number of arterioles, and supposedly of aBV. The present results suggest that there is an increase in aBV in tumours, potentially proportional to the increase in the number of arterioles, since the highest values of aBV were found in tumours with the highest malignancy grade (glioblastoma) and the highest vascularity according to histology (meningiomas). Also, an increase in ratio and value of aBV was accompanied by an increase in ratio and value of DSC-CBV, respectively (Figure 3a and 4a). Hence, it may be suggested that elevated aBV in the tumour is a measure of malignancy similar to the DSC-CBV parameter. Previous reports on arterial blood volume in tumours are scarce. In a material of 22 benign, malignant and intermediate ovarian tumours, the fraction of arterioles in the microcirculation (defined as the number of arterioles divided by the sum of arterioles and venules) was significantly lower in the malignant (0.3) than in the benign tumours (0.56) [31]. Simultaneously the vascular density (defined as the overall number of arterioles and venules) was higher in the malignant than in the benign tumours. This suggests that the increase in CBV is due to a proportionally larger increase in the venous than in the arterial blood volume in malignant tumours and may explain the findings in the present study that aBV and CBV did not correlate as well as ASL-CBF and DSC-CBF ratios. This may also explain the larger increase in CBV than in aBV when going from grade III gliomas to glioblastomas. Large scale studies on the arterial and venous blood volume in tumours are needed to clarify this issue further. Another aspect influencing the aBV is the possibility that a small fraction of the protons included in the aBV during measurement may have recirculated into the venules resulting in a slight overestimation of the true arterial

blood volume. A study on tumour blood flow in meningiomas using ASL and DSC-MRI showed a good correlation between the two techniques ($R^2$ = 0.73) [32].

Although the aim of the present study was to investigate the correlation between aBV and CBV in intracranial tumours as a first step in the process of evaluating the use of aBV as a tool for tumour grading similar to existing CBV-based methods, a brief comparison with previous investigations of comparable aim is reasonable. CBF ratios obtained by ASL and DSC-MRI in low-grade (2.16 and 2.23, respectively) and high grade gliomas (3.45 and 2.69, respectively) were considerably higher in the present study than in a previous work that studied 29 gliomas grade I-IV (0.64 and 0.6, respectively, in low-grade and 1.54 and 1.28, respectively, in high-grade gliomas) [24]. Tumour-to-GM CBF ratios obtained from ASL Q2TIPS in 35 patients with, amongst others, gliomas, meningiomas and schwannomas have been reported to be 1.5 for low-grade gliomas and 2.5 for high grade gliomas [33], to be compared with 2.16 and 3.45 for grade III gliomas and glioblastomas, respectively, in the present study. Reports also include CBF from continuous ASL, in high-grade and low-grade gliomas [26], where glioma grading was based on the mean and maximum tumour blood flow and these measures were normalized to global CBF. The normalized values (2.8 in high-grade and 1.1 in low-grade gliomas) provided the best distinction between high-grade and low-grade gliomas. This suggests that our data obtained using QUASAR /DSC may be satisfactorily compared with those from CASL/DSC and Q2TIPS/DSC. We may thus conclude that a trend can be observed towards high-grade gliomas demonstrating a larger tumour-to-GM aBV ratio than low grade tumours and that large scale studies including a larger number of patients are needed to evaluate the usefulness of aBV as a measure of malignancy.

Tumour-to-WM ratios of DSC-CBF and DSC-CBV in brain tumours have been frequently reported. One study found ratios of 6.50 ± 4.29 and 3.32 ± 1.87 (mean±SD) for DSC-CBF and DSC-CBV, respectively, in high grade gliomas and of 1.69 ± 0.51 and 1.16 ± 0.38, respectively, in low-grade gliomas [35]. Average ratios of tumour-to-healthy tissue CBV have been reported to be 3.64 [5], 5.07 [6], 5.18 [35] and 4.91 [36] in high-grade gliomas and 1.11 [5], 1.44 [6], 2.14 [36] and 2.00 [36] in low-grade gliomas. Measurements of CBV in healthy tissue, however, can differ between studies. The values above are to be compared with median values of 1.46

for grade III gliomas and 3.89 for glioblastomas in the present study including rather few individuals in each group.

Both ASL and DSC-MRI perfusion measurements have their strengths and weaknesses. The main methodological problems with QUASAR are low signal-to-noise ratio, limited temporal resolution and artefacts due to head movements. However, with respect to CBF, the method has proven a reasonable repeatability of 13.0 [ml/100 g/min]) in a study where 284 healthy volunteers (average age 33 years) at 28 sites world-wide were scanned four times each during a two-week period, with and without repositioning [22]. Also, in a study comparing CBF in healthy grey matter using DSC-MRI and QUASAR the correlation between the two modalities was very good (r=0.89) [21]. In our study, ASL-CBF was 41 ml/(min 100 g), while gold standard CBF techniques typically report GM CBF values in the order of 60-80 mL/(min 100 g). In previous studies using the QUASAR technique for ASL-CBF measurement, values of 47.4 ± 7.5 [ml/ 100 g/min] [22] and 40.2 ± 6.9 ml/(min 100 g) [37] were found. Hence, the values found in the present work are well in accordance with previous QUASAR studies.

At present, measurement of aBV is relatively time consuming (roughly 5 min vs. 1.5 min for DSC-CBV), the spatial resolution is relatively crude (3.75 $mm^2$ vs 1.7 $mm^2$) and the spatial coverage is clearly reduced (56 mm vs. 138 mm) in comparison with a DSC-CBV measurement. Although this is to some extent compensated for by the complete non-invasiveness of ASL, these factors certainly hamper the use of aBV in clinical routine examinations. Therefore, further technical developments are required in order for aBV to become a widely available clinical tool. A major concern regarding the use of DSC-MRI for monitoring angiogenesis is the leakage of contrast agent from the vasculature to the tumour during measurement, resulting in inaccurate CBV values. Attempts to correct DSC-CBV estimates in regions of microvascular leakage include pre-injection of a small amount of contrast agent to temporarily saturate the tissue T1-relaxation, use of dual-echo pulse sequences and baseline subtraction, but none is considered to be the standard method of choice. In spite of this, DSC-CBV measurements have been shown to correlate reliably with tumour grade and histologic findings of increased tumour vascularity [5-8, 38]. Finally, the observed correlation between ASL-aBV and DSC-CBV ratios may also have been

influenced by methodological factors, characteristic for each of the employed techniques. For example, vascular architecture is likely to differ between tumours and normal tissue, and DSC results may thus be influenced by the effects of vascular architecture on T2* relaxivity [39]. Similarly, the velocity distribution could be different in tumour tissue, and this would hamper a direct comparison between aBV estimates in tumour and normal tissue due to the use of a fixed velocity threshold in the QUASAR sequence. These potential contributions to our results were not assessed separately.

In our study, the average CBF ratio obtained using ASL was similar to, but slightly higher than, the CBF ratio obtained using DSC-MRI. Model-free ASL provides somewhat low GM CBF estimates, presumably because crusher gradients eliminate signal from fast-flowing blood in the arteries and arterioles, included in other perfusion imaging modalities. However, in the tumour the blood-flow velocity may be lower and thus is not crushed to the same extent.

**Conclusion:**

In conclusion, aBV data obtained from ASL correlated well with CBV data obtained from DSC-MRI, both with regard to tumour-to-GM ratios and parametric values, when a 4-pixel ROI representing the maximal tumour values was used. Our results suggest that measurement of aBV has a potential for non-invasive assessment of blood volume in intracranial tumours.

**Acknowledgments:**

This study was supported by the Swedish Cancer Society (grant no. 070198), the Skåne County Council Research and Development Foundation, the Crafoord Foundation and the Swedish Research Council (grants no. 13514, 2007-3974, 2007-6079 and 2008-3183)

**References**


1. Wesseling P, Ruiter DJ, Burger PC (1997) Angiogenesis in brain tumors; pathobiological and clinical aspects. J Neurooncol. 32:253-65.
2. Plate KH Mennel HD (1995) Vascular morphology and angiogenesis in glial tumors. Exp Toxicol Pathol 47:89–94.
3. Rampling R, Cruickshank G, Lewis A, Fitzsimmon S, Workman, P (1994) Direct measurement of pO-distribution and bioreductive enzymes in human malignant brain tumors. Int. J. Radiat Oncol Biol Phys 29:427–431.
4. Valk, PE, Mathis, CA, Prados MD, Gilbert JC, Budinger, TF (1992) Hypoxia in human gliomas: demonstration by PET with fluorine-18fluoromisonidazole. J Nucl Med 33:2133–2137.
5. Aronen HJ, Gazit IE, Louis DN, Aronen HJ, Gazit IE, Louis DN, Buchbinder BR, Pardo FS, Weisskoff RM, Harsh GR, Cosgrove GR, Halpern EF, Hochberg FH, Rosen BR (1994) Cerebral blood volume maps of gliomas: comparison with tumor grade and histologic findings. Radiology 191: 41–51.
6. Knopp EA, Cha S, Johnson G, Mazumdar A, Golfinos JG, Zagzag D, Miller DC, Kelly PJ, Kricheff II (1999) Glial neoplasms: dynamic contrast-enhanced T2*-weighted MR imaging. Radiology 211:791–98.
7. Sugahara T, Korogi Y, Kochi M, Ikushima I, Shigematu Y, Hirai T, Okuda T, Liang L, Ge Y, Komohara Y, Ushio Y, Takahashi M (1998) Correlation of MR imaging-determined cerebral blood volume maps with histologic and angiographic determination of vascularity of gliomas. AJR Am J Roentgenol 171:1479 – 86.
8. Lev MH, Ozsunar Y, Henson JW, Rasheed AA, Barest GD, Harsh GR 4th, Fitzek MM, Chiocca EA, Rabinov JD, Csavoy AN, Rosen BR, Hochberg FH, Schaefer PW, Gonzalez RG (2004) Glial tumor grading and outcome prediction using dynamic spin-echo MR susceptibility mapping compared with conventional contrast-enhanced MR: confounding effect of elevated rCBV of oligodendrogliomas. AJNR Am J Neuroradiol 25:214 –21.
9. Zierler KL (1962) Theoretical basis of indicator-dilution methods for measuring flow and volume. Circ Res 10:393– 407.
10. Williams DS, Detre JA, Leigh JS, Koretsky AP (1992) Magnetic resonance imaging of perfusion using spin inversion of arterial water. Proc Natl Acad Sci U S A. 1992:89:212-216. Erratum in: Proc Natl Acad Sci U S A 89:4220.

11. Detre JA, Leigh JS, Williams DS, Koretsky AP (1992) Perfusion imaging. Magn Reson Med 23:37-45.
12. Edelman RR, Siewert B, Darby DG, Thangaraj V, Nobre AC, Mesulam MM, Warach S (1994) Qualitative mapping of cerebral blood flow and functional localization with echo-planar MR imaging and signal targeting with alternating radio frequency. Radiology 192:513-520.
13. Kim SG (1995) Quantification of relative cerebral blood flow change by flow-sensitive alternating inversion recovery (FAIR) technique: application to functional mapping. Magn Reson Med 34:293-301.
14. Petersen ET, Lim T, Golay X (2006) Model-free arterial spin labelling quantification approach for perfusion MRI. Magn Reson Med 55:219-232.
15. Peak AS, Sheller A (2007) Risk factors for developing gadolinium-induced nephrogenic systemic fibrosis. Ann Pharmacother 41:1481-5.
16. Wu O, Østergaard L, Weisskoff RM, Benner T, Rosen BR, Sorensen AG (2003) Tracer arrival timing-insensitive technique for estimating flow in MR perfusion-weighted imaging using singular value decomposition with a block-circulant deconvolution matrix. Magn Reson Med 50:164-74.
17. Rempp KA, Brix G, Wenz F, Becker CR, Gückel F, Lorenz WJ (1994) Quantification of regional cerebral blood flow and volume with dynamic susceptibility contrast-enhanced MR imaging. Radiology 193:637-641.
18. Boxerman JL, Schmainda KM, Weisskoff RM (2006) Relative cerebral blood volume maps corrected for contrast agent extravasation significantly correlate with glioma tumor grade, whereas uncorrected maps do not. AJNR Am J Neuroradiol 27:859-67.
19. Wetzel SG, Cha S, Johnson G, Lee P, Law M, Kasow DL, Pierce SD, Xue X (2002) Relative cerebral blood volume measurements in intracranial mass lesions: interobserver and intraobserver reproducibility study. Radiology 224:797-803.
20. Knutsson L, van Westen D, Petersen ET, Markenroth Bloch K, Holtås S, Ståhlberg F, Wirestam R (2010) Absolute quantification of cerebral blood flow using dynamic susceptibility contrast MRI: a comparison with model-free arterial spin labeling. Magn Reson Imaging 28:1-7.
21. Petersen ET, Mouridsen K, Golay X, on behalf of all named coauthors of the QUASAR test-retest study (2010) The QUASAR reproducibility study, Part II:

Results from a multi center Arterial Spin Labeling test-retest Study. Neuroimage. 1;49(1):104-13.

22. Di Chiro G, Brooks R, Bairamian D (1985) Diagnostic and prognostic value of positron emission tomography using [‘8Fl fluorodepxyglucose in brain tumors. In: Reivich M, Alavi A, eds. Positron emission tomography. New York, NY: Alan R. Liss, 291-309.
23. Law M, Oh S, Babb JS, Wang E, Inglese M, Zagzag D, Knopp EA, Johnson G (2006) Low-grade gliomas: dynamic susceptibility weighted contrast-enhanced perfusion MR imaging – prediction of patient clinical response. Radiology 238:658 – 67.
24. Warmuth C, Gunther M, Zimmer C (2003) Quantification of blood flow in brain tumors: Comparison of arterial spin labeling and dynamic susceptibility-weighted contrast-enhanced MR imaging. Radiology 228:523 –532.
25. Weber MA, Zoubaa S, Schlieter M, Jüttler E, Huttner HB, Geletneky K, Ittrich C, Lichy MP, Kroll A, Debus J, Giesel FL, Hartmann M, Essig M (2006) Diagnostic performance of spectroscopic and perfusion MRI for distinction of brain tumors. Neurology 66:1899 –1906.
26. Wolf RL, Wang J, Wang S, Melhem ER, O'Rourke DM, Judy KD, Detre JA. (2005) Grading of CNS neoplasms using continuous arterial spin labeled perfusion MR imaging at 3 Tesla. J Magn Reson Imaging 22:475 – 482.
27. Weber MA, Thilmann C, , Günther M, Delorme S, Zuna I, Bongers A, Schad LR, Debus J, Kauczor HU, Essig M, Schlemmer HP (2004) Assessment of irradiated brain metastases by means of arterial spin-labeling and dynamic susceptibility-weighted contrast-enhanced perfusion MRI: initial results. Invest Radiol 39:277-87.
28. Kahle, Leonhardt, Platzer (2004) Color Atlas and Textbook of Human Anatomy: Internal Organs. Stuttgart, Germany: Thieme Medical Publishers; 5th revised edition.
29. Ito H, Kanno I, Iida H, Hatazawa J, Shimosegawa E, Tamura H, Okudera T (2001) Arterial fraction of cerebral blood volume in humans measured by positron emission tomography. Ann Nucl Med. 15:111-6.
30. Kidron D, Bernheim J, Aviram R, Cohen I, Fishman A, Beyth Y, Tepper R (1999) Resistance to blood flow in ovarian tumors: correlation between resistance

index and histological pattern of vascularization. Ultrasound Obstet Gynecol. 13:425-30.

31. Kimura H, Takeuchi H, Koshimoto Y, Arishima H, Uematsu H, Kawamura Y, Kubota T, Itoh H (2006) Perfusion imaging of meningioma by using continuous arterial spin-labeling: comparison with dynamic susceptibility-weighted contrast-enhanced MR images and histopathologic features. AJNR Am J Neuroradiol. 27:85-93.
32. Noguchi T, Yoshiura T, Hiwatashi A, Togao O, Yamashita K, Nagao E, Shono T, Mizoguchi M, Nagata S, Sasaki T, Suzuki SO, Iwaki T, Kobayashi K, Mihara F, Honda H (2008) Perfusion imaging of brain tumors using arterial spin-labeling: correlation with histopathologic vascular density. AJNR Am J Neuroradiol. 29:688-93.
33. Hakyemez B, Erdogan C, Ercan I, Ergin N, Uysal S, Atahan S (2005) High-grade and low-grade gliomas: differentiation by using perfusion MR imaging. Clin Radiol. 60:493-502.
34. Law M, Yang S, Wang H, Babb JS, Johnson G, Cha S, Knopp EA, Zagzag D (2003) Glioma grading: sensitivity, specificity, and predictive values of perfusion MR imaging and proton MR spectroscopic imaging compared with conventional MR imaging. AJNR Am J Neuroradiol 24 :1989–98.
35. Shin JH, Lee HK, Kwun BD, Kim JS, Kang W, Choi CG, Suh DC (2002) Using relative cerebral blood flow and volume to evaluate the histopathological grade of cerebral gliomas: preliminary results. AJR Am J Roentgenol 179 :783–9
36. Uchihasi Y, Hosoda K, Zimine I, Fujita A, Inoue S, Aihara H, Kawamitsu H, Aoyama N, Aoki A, Fjii M, Kohmura E (2009). Comparison of CBF measurement by ASL and SPECT in patients with internal carotid artery stenosis. In: Proceedings of the 17th Annual Meeting of ISMRM, Honolulu, Hawaii (abstract 34)
37. Aronen H, Pardo FS, Kennedy DN, Belliveau JW, Packard SD, Hsu DW, Hochberg FH, Fischman AJ, Rosen BR (2000) High microvascular blood volume is associated with high glucose uptake and tumor angiogenesis in human gliomas. Clin Cancer Res 6:2189–2200.
38. Kjølby BF, Østergaard L, Kiselev VG (2006) Theoretical model of intravascular paramagnetic tracers effect on tissue relaxation. Magn Reson Med 56:187-197.

**Table 1**

Tumour-to-GM ratios (group median and range) for the four perfusion parameters per tumour type, (a) for the 4-pixel ROI representing the maximum value in the tumour and (b) for a ROI covering the entire tumour in the same slice

| **a. Tumour-to-GM ratios for the 4-pixel ROI, median and range** | | | | |
|---|---|---|---|---|
| | **ASL-aBV** | **DSC-CBV** | **ASL-CBF** | **DSC-CBF** |
| **Glioma gr III** (n=3) | 1.06 (0.12 - 2.17) | 1.46 (0.67 – 2.92) | 2.16 (0.36 – 2.41) | 2.23 (0.56 – 2.83) |
| **Glioblastoma** (n=4) | 2.00 (0.78 - 3.08) | 3.89 (1.98 – 4.31) | 3.45 (2.11 – 4.47) | 2.69 (2.40 - 4.48) |
| **Meningioma** (n=4) | 2.81 (1.35 - 3.85) | 7.90 (3.46 – 8.95) | 6.91 (3.79 - 7.40) | 6.34 (2.23 – 7.57) |
| | | | | |
| **b. Tumour-to-GM ratios for the whole tumour (1 slice), median and range** | | | | |
| | **ASL-aBV** | **DSC-CBV** | **ASL-CBF** | **DSC-CBF** |
| **Glioma gr III** (n=3) | 0.98 (0.10 – 2.74) | 1.19 (0.80 – 2.45) | 0.72 (0.39 – 1.10) | 1.44 (0.48 – 1.58) |
| **Glioblastoma** (n=4) | 1.34 (1.00 – 3.01) | 2.60 (1.10 – 3.22) | 1.35 (0.55 – 2.11) | 1.57 (0.83 – 3.69) |
| **Meningioma** (n=4) | 1.58 (0.61 – 1.92) | 4.25 (2.02 – 7.28) | 4.36 (2.30 – 6.89) | 3.95 (1.43 – 5.42) |
| | | | | |

**Table 2**

Values (median and range) of each parameter per tumour type determined as (a) the maximum tumour value in a 4-pixel ROI and (b) the value in the entire tumour in one slice, as well as (c) values of each parameter in healthy grey matter. Note that DSC-based estimates are systematically overestimated, and should be regarded as indices rather than true absolute values.

| **a. Maximum value in a 4-pixel ROI, median and range** | | | | |
|---|---|---|---|---|
| | **ASL-aBV** (%) | **DSC-CBV** ml/100 g | **ASL-CBF** ml/(min 100g) | **DSC-CBF** ml/(min 100 g) |
| **Glioma gr III** (n=3) | 1.12 (0.12 – 2.45) | 83 (32- 172) | 94 (15 – 115) | 1293 (275 – 2345) |
| **Glioblastoma** (n=4) | 1.91 (0.56 – 2.89) | 179 (101 – 289) | 108 (89 – 114) | 1536 (962 – 1747) |
| **Meningioma** (n=4) | 2.17 (1.46 – 3.43) | 347 (159 – 385) | 269 (97 – 303) | 2879 1275 – 3295) |
| | | | | |
| **b. Values in entire tumour in one slice, median and range** | | | | |
| | **ASL-aBV (%)** | **DSC-CBV** *ml/100 g* | **ASL-CBF** *ml/(min 100g)* | **DSC-CBF** *ml/(min 100 g)* |
| **Glioma gr III** (n=3) | 1.03 (0.09 – 1.98) | 61 (30 – 105) | 31 (13 – 45) | 834 (235 – 1315) |
| **Glioblastoma** (n=4) | 1.47 (0.75 – 1.81) | 132 (62 – 139) | 52 (24 – 97) | 902 (322 – 1437) |
| **Meningioma** (n=4) | 1.51 (0.66 – 1.94) | 235 (92 – 276) | 146 (58 – 189) | 834 (815 – 2358) |
| | | | | |
| **c. Values in healthy grey matter** | | | | |
| **All patients** (n=11) | 0.95 (0.75 –1.13) | 46 (38 - 67) | 41 (26 – 48) *)* | 495 (390-830) |

**Table 3 Parametric values (average of the pixel values in the 4 pixel ROI, top, and in the ROI covering the whole tumour, bottom) and standard deviations in these ROIs (absolute value and percentage of the average ROI value).** Note that DSC-based estimates are systematically overestimated, and should be regarded as indices rather than true absolute values.

| | | ASL_aBV (%) | | | DSC_CBV | | | ASL_CBF | | | DSC_CBF | | |
|---|---|---|---|---|---|---|---|---|---|---|---|---|---|
| **4-pixel ROI** | | **average** | **stdev** | **st dev %** | **average** | **stdev** | **st dev %** | **average** | **stdev** | **st dev %** | **average** | **stdev** | **st dev %** |
| | | (%) | | | ml/100 g | | | ml/(min 100g) | | | ml/(min 100g) | | |
| 1/47/M | Glioma gr III | 0.12 | 0.04 | 41% | 32 | 8 | 24% | 16 | 4 | 24% | 275 | 18 | 7% |
| 5/46/M | Glioma gr III | 1.12 | 0.32 | 29% | 83 | 12 | 16% | 94 | 9 | 13% | 1293 | 48 | 4% |
| 7/48/F | Glioma gr III | 2.45 | 0.47 | 19% | 172 | 24 | 14% | 115 | 9 | 8% | 2412 | 333 | 14% |
| 2/48/F | Glioma gr IV | 1.52 | 0.27 | 18% | 289 | 46 | 17% | 114 | 12 | 11% | 1706 | 100 | 6% |
| 3/58/M | Glioma gr IV | 2.30 | 0.21 | 9% | 221 | 31 | 14% | 114 | 12 | 10% | 1747 | 116 | 7% |
| 6/34/F | Glioma gr IV | 2.89 | 0.41 | 15% | 138 | 147 | 15% | 101 | 5 | 5% | 962 | 147 | 15% |
| 9/35/M | Glioma gr IV | 0.56 | 0.24 | 44% | 101 | 16 | 17% | 89 | 9 | 11% | 1366 | 168 | 12% |
| 4/60/F | Meningioma | 1.46 | 0.02 | 2% | 159 | 27 | 17% | 97 | 7 | 8% | 1275 | 185 | 14% |
| 8/64/F | Meningioma | 1.85 | 0.26 | 15% | 357 | 49 | 16% | 259 | 18 | 7% | 2615 | 353 | 13% |
| 10/67/F | Meningioma | 2.50 | 0.17 | 7% | 385 | 54 | 16% | 280 | 22 | 8% | 3295 | 199 | 7% |
| 10/67/F | Meningioma | 3.43 | 0.40 | 12% | 338 | 8 | 2% | 303 | 34 | 11% | 3143 | 331 | 10% |
| | median | | | 15% | | | 16% | | | 10% | | | 10% |
| **Whole tumour ROI** | | | | | | | | | | | | | |
| 1/47/M | Glioma gr III | 0.10 | 0.10 | 104% | 31 | 10 | 32% | 13 | 11 | 80% | 236 | 66 | 28% |
| 5/46/M | Glioma gr III | 1.99 | 1.45 | 73% | 61 | 24 | 40% | 30 | 17 | 57% | 834 | 242 | 29% |
| 7/48/F | Glioma gr III | 1.14 | 1.01 | 89% | 105 | 40 | 38% | 45 | 28 | 61% | 1315 | 371 | 28% |
| 2/48/F | Glioma gr IV | 1.83 | 0.82 | 45% | 125 | 67 | 53% | 98 | 38 | 38% | 1151 | 420 | 36% |
| 3/58/M | Glioma gr IV | 0.75 | 0.58 | 78% | 139 | 64 | 46% | 78 | 34 | 43% | 1437 | 647 | 45% |
| 6/34/F | Glioma gr IV | 1.81 | 0.35 | 19% | 138 | 14 | 10% | 27 | 23 | 85% | 332 | 196 | 59% |
| 9/35/M | Glioma gr IV | 1.12 | 0.34 | 30% | 63 | 36 | 57% | 24 | 22 | 89% | 655 | 402 | 61% |
| 4/60/F | Meningioma | 0.66 | 0.50 | 75% | 93 | 30 | 32% | 59 | 16 | 26% | 816 | 254 | 31% |
| 8/64/F | Meningioma | 1.50 | 0.56 | 37% | 277 | 79 | 28% | 189 | 40 | 21% | 1753 | 494 | 28% |
| 10/67/F | Meningioma | 1.94 | 0.42 | 22% | 250 | 68 | 27% | 164 | 60 | 37% | 2358 | 647 | 27% |
| 10/67/F | Meningioma | 1.53 | 0.84 | 55% | 221 | 68 | 31% | 127 | 72 | 57% | 1845 | 647 | 35% |
| | median | | | 55% | | | 32% | | | 57% | | | 31% |

## Figure Legends

### Figure 1

Gadolinium enhanced T1-weighted image, the corresponding aBV map from ASL and CBV map from DSC-MRI as well as CBF maps from ASL and DSC-MRI are displayed with the contrast enhancing meningioma outlined by a rectangle. Within the tumour were multiple ROIs of 4 pixels (11.8 $mm^2$) placed in each parametric map in order to obtain the highest value and determine its ratio to healthy grey matter. Tumour-to-GM ratios for ASL-aBV and DSC-CBV were 2.48 and 7.93 respectively, and for ASL-CBF and DSC-CBF 7.0 and 5.45, respectively.

### Figure 2

Gadolinium enhanced T1-weighted image, the corresponding aBV map from ASL and CBV map from DSC-MRI as well as CBF maps from ASL and DSC-MRI are displayed with the contrast enhancing glioblastoma partly outlined by a rectangle. Within the tumour were multiple ROIs of 4 pixels (11.8 $mm^2$) placed in each parametric map in order to obtain the highest value and determine its ratio to healthy grey matter. Tumour-to-GM ratios for ASL-aBV and DSC-CBV were 1.60 and 4.31, respectively, and for ASL-CBF and DSC-CBF the ratios were 2.89 and 4.47, respectively.

### Figure 3

a. Tumour-to-healthy grey matter ratios for ASL-aBV and DSC-CBV in the 4-pixel ROI with the tumour maximum, coefficient of determination $R^2 = 0.61$, $P = 0.0045$.
b. Tumour-to-healthy grey matter ratios for ASL-CBF and DSC-CBF in the 4-pixel ROI with the tumour maximum, coefficient of determination $R^2 = 0.86$, $P = 0.0001$.
c. Tumour-to-healthy grey matter ratios for ASL-aBV and DSC-CBV in the ROI covering the entire tumour, coefficient of determination $R^2 = 0.25$, $P = 0.12$.

**Figure 4**

Note that DSC-based estimates are systematically overestimated, and should be regarded as indices rather than true absolute values.

a. Parametric values for ASL-aBV and DSC-CBV in the 4-pixel ROI with the tumour maximum, coefficient of determination without proportionality $R^2$ = 0.37, *P* = 0.049
b. Parametric values for ASL-CBF and DSC-CBF in the 4-pixel ROI with the tumour maximum, coefficient of determination without proportionality $R^2$ = 0.86, *P* < 0.0001
c. Parametric values for ASL-aBV and DSC-CBV in the ROI covering the entire tumour, coefficient of determination without proportionality $R^2$ = 0.16, *P* = 0.22.

**Figure 5**

a. Comparison between lesion-to-brain ratios of ASL-aBV and DSC-CBV measured in the 4-pixel area with the maximum ASL-aBV, coefficient of determination without proportionality $R^2$ = 0.56, *P* = 0.008.
b. Comparison between lesion-to-brain ratios of ASL-aBV and DSC-CBV measured in the 4-pixel area with the maximum DSC-CBV, coefficient of determination without proportionality $R^2$ = 0.51, *P* = 0.014.
c. Comparison between parametric values of ASL-aBV and DSC-CBV measured in the 4-pixel area with the maximum ASL-aBV, coefficient of determination without proportionality $R^2$ = 0.37, *P* = 0.053.
d. Comparison between parametric values of ASL-aBV and DSC-CBV measured in the 4-pixel area with the maximum DSC-CBV, coefficient of determination without proportionality $R^2$ = 0.33, *P* = 0.01.

In c and d, note that DSC-based estimates are systematically overestimated, and should be regarded as indices rather than true absolute values.

**Figure 1**

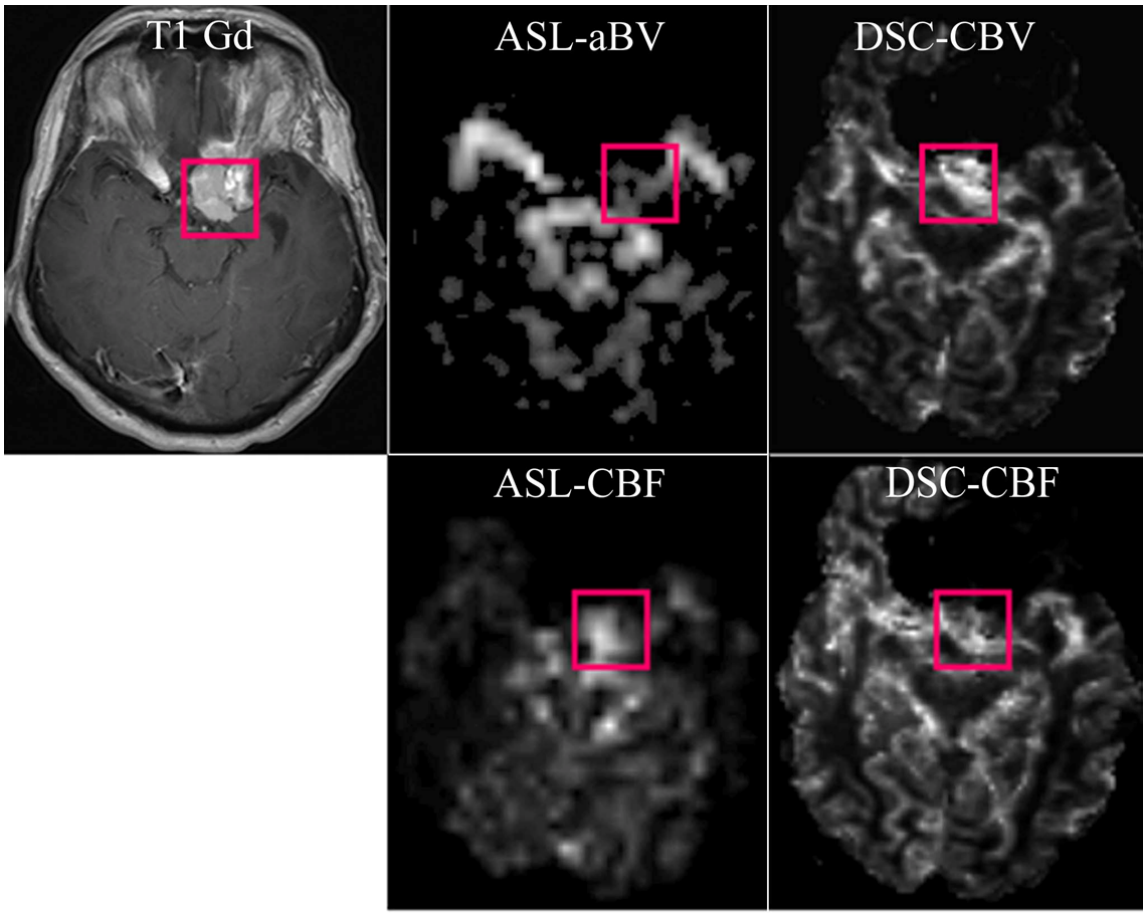

Figure 2

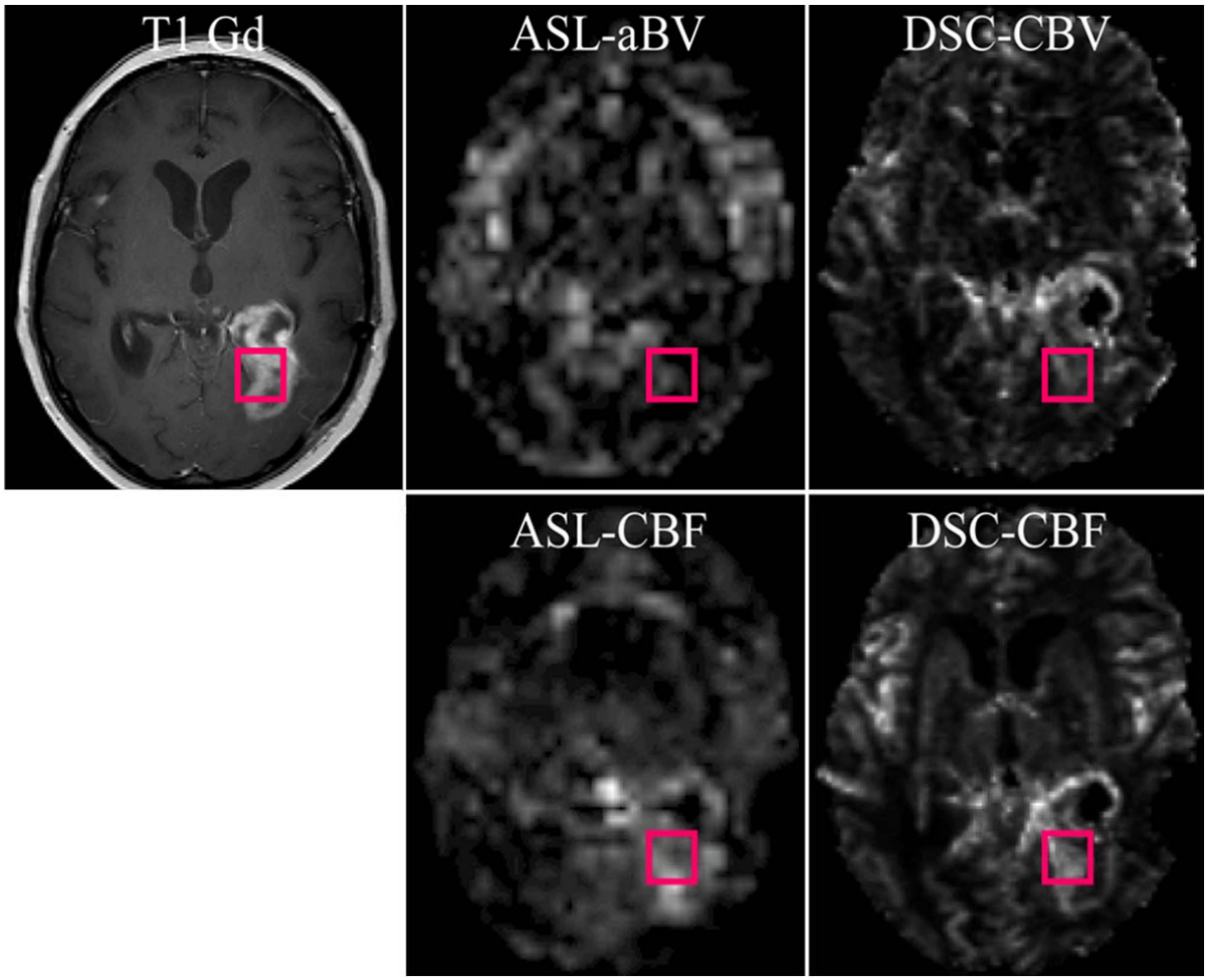

**Figure 3**

a. Tumour-to-healthy grey matter ratios for ASL-aBV and DSC-CBV in the 4-pixel ROI with the tumour maximum, coefficient of determination $R^2 = 0.61$, $P = 0.0045$

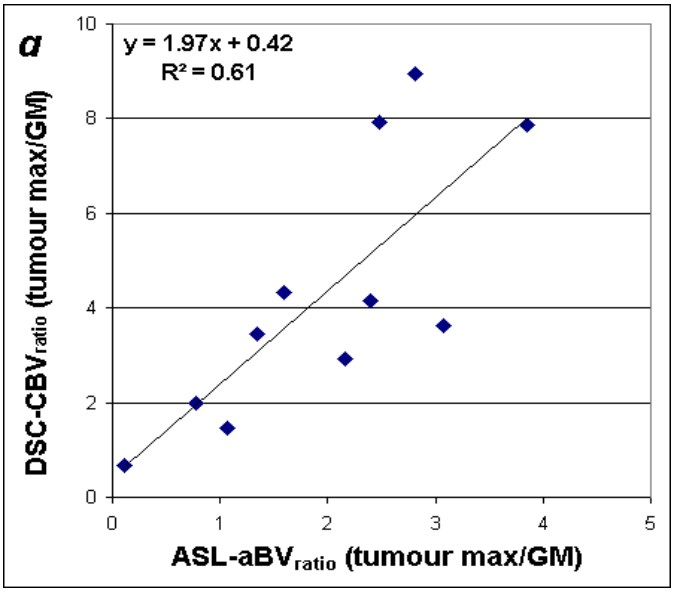


b.

Tumour-to-healthy grey matter ratios for ASL-CBF and DSC-CBF in the 4-pixel ROI with the tumour maximum, coefficient of determination $R^2 = 0.86$, $P = 0.0001$.

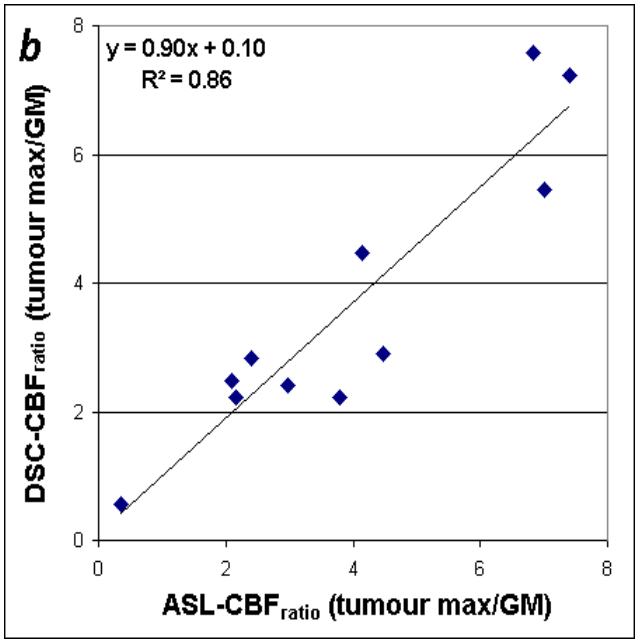

c.

Tumour-to-healthy grey matter ratios for ASL-aBV and DSC-CBV in the ROI covering the entire tumour, coefficient of determination without proportionality $R^2 = 0.25$, $P = 0.12$.

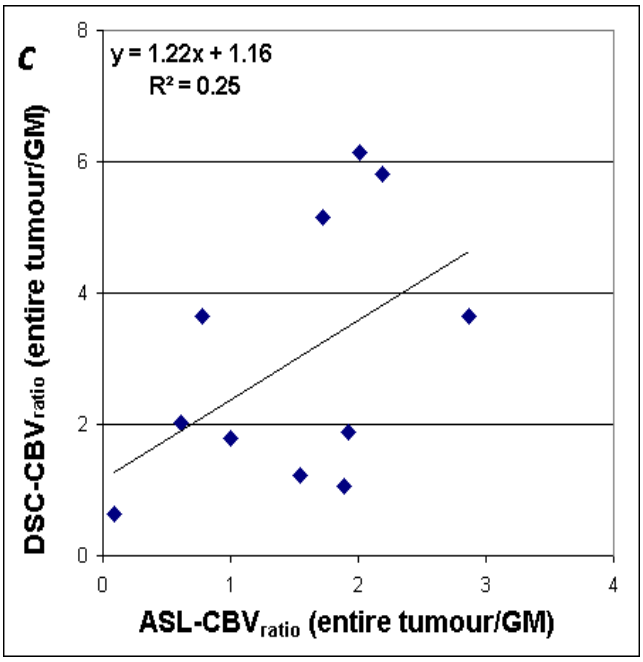

**Fig 4**

Note that DSC-based estimates are systematically overestimated, and should be regarded as indices rather than true absolute values.

a.

Parametric values for ASL-aBV and DSC-CBV in the 4-pixel ROI with the tumour maximum, coefficient of determination without proportionality $R^2 = 0.37$, $P = 0.049$.

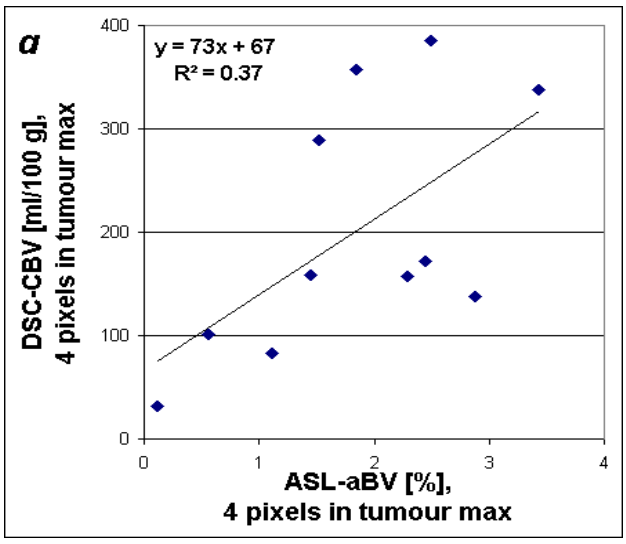


b. Parametric values for ASL-CBF and DSC-CBF in the 4-pixel ROI with the tumour maximum, coefficient of determination without proportionality $R^2 = 0.86$, $P < 0.0001$.

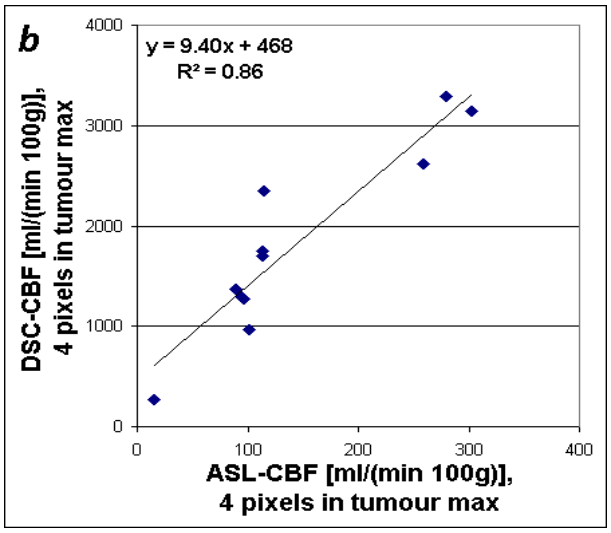

c.

Parametric values for ASL-aBV and DSC-CBV in the ROI covering the entire tumour, coefficient of determination without proportionality $R^2 = 0.16$, $P = 0.22$.

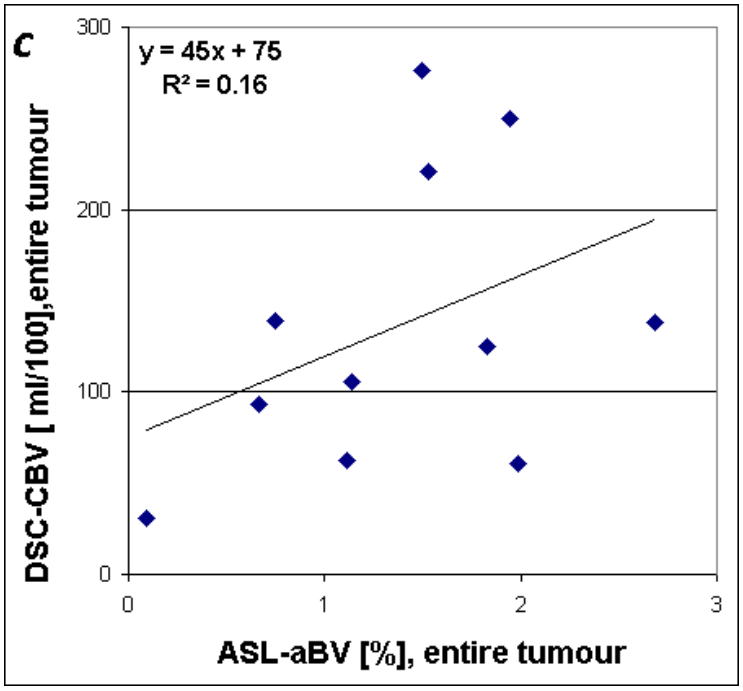

**Fig 5**

**a.**

Comparison between lesion-to-brain ratios of ASL-aBV and DSC-CBV measured in the 4-pixel area with the maximum ASL-aBV, coefficient of determination without proportionality $R^2$= 0.56, *P* = 0.008.

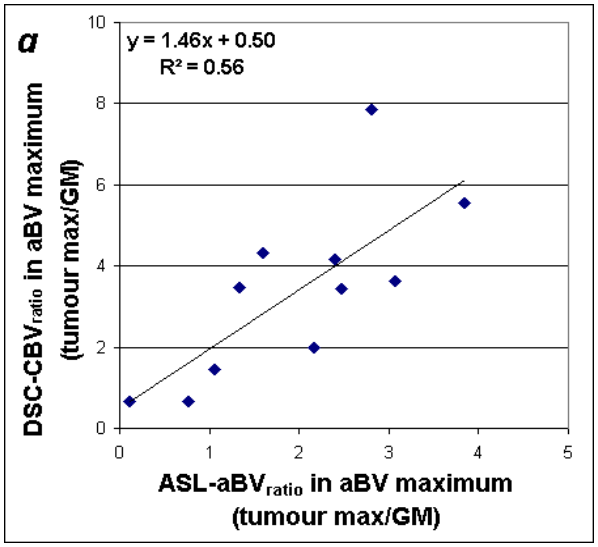


**b.**Comparison between lesion-to-brain ratios of ASL-aBV and DSC-CBV measured in the 4-pixel area with the maximum DSC-CBV, coefficient of determination without proportionality $R^2$ = 0.51, *P* = 0.014.

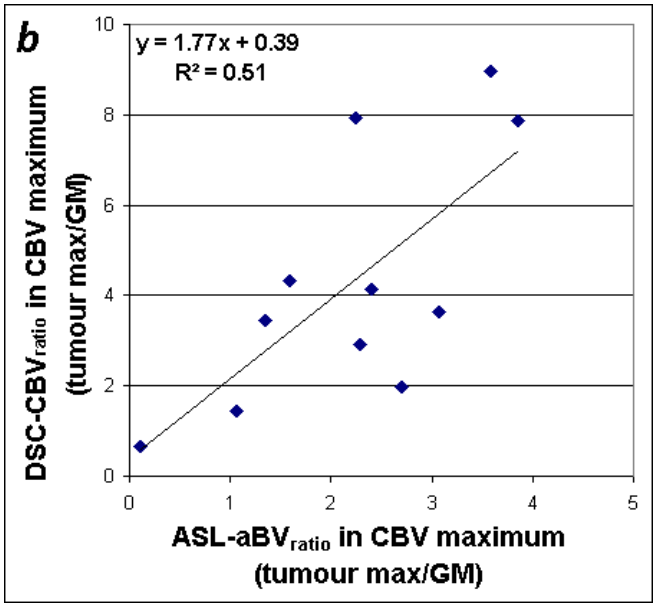

**c.** Comparison between parametric values of ASL-aBV and DSC-CBV measured in the 4-pixel area with the maximum ASL-aBV, coefficient of determination without proportionality $R^2 = 0.37$, $P = 0.053$.

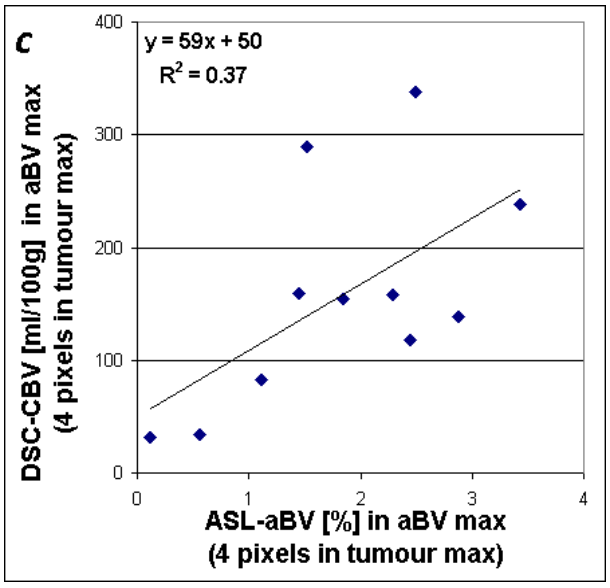


**d.**

Comparison between parametric values of ASL-aBV and DSC-CBV measured in the 4-pixel area with the maximum DSC-CBV, coefficient of determination without proportionality $R^2 = 0.33$, $P = 0.0$